Ultra-Wide Range Refractive Index PCF-Based SPR Sensor for Lab-on-Chip Applications

Ruhul Amin
Dept. of Electrical and Electronic Engineering
Bangladesh University of Business and Technology (BUBT)
Dhaka-1216, Bangladesh
ruhulamin876@gmail.com

Nam-Phong Nguyen
School of Electronics and Telecommunication
Hanoi University of Science and Technology
Hanoi, Vietnam
nguyennamphong1989@gmail.com

Md. Anwar Hossain
Dept. of Electrical and Electronic Engineering
Bangladesh University of Business and Technology (BUBT)
Dhaka-1216, Bangladesh
anwar.ee113@ieee.org

Abdullah Saleh
Dept. of Electrical and Electronic Engineering
Ahsanullah University of Science and Technology (AUST)
Dhaka-1208, Bangladesh
abdullah.saleh546@gmail.com

Nguyen Hoang Hai
School of Electronics and Telecommunication
Hanoi University of Science and Technology
Hanoi, Vietnam
hai.nguyenhoang@hust.edu.vn

***Abstract*— Using finite element method, a novel photonic crystal fiber (PCF) based surface plasmon resonance (SPR) sensor, capable of detecting multiple samples simultaneously, is designed and analyzed in this paper. Applying perfectly matched layer boundary condition, maximum wavelength sensitivity of 22,000 nm/RIU, amplitude sensitivity of 1629 RIU^{-1} and an ultra-wide range refractive index (RI) from 1.17 to 1.43, are reported for detecting gaseous and liquid materials. These features will open to design, analyze, fabricate, and test Lab-on-Chip (LOC) devices for plant science, food safety, environment analysis, and medical diagnosis.**

Keywords*— *Lab-on-chip, wavelength sensitivity, amplitude sensitivity, SPR sensor.

I. INTRODUCTION

Photonic crystal fiber (PCF) based surface plasmonic resonance (SPR) sensor has become a promising research field for researchers due to the outstanding tunable optical properties of PCFs, wide sensing ranges, and comprehensive applications including environment monitoring, gas detection, disease detection, bio-imaging, bio-medical, bioengineering, chemical sensing, and so on [1]. Very recently, researchers have been thinking about designing a unique sensor chip using novel LOC technology that will be useable for medical diagnosis, food safety, plant science, and environmental analysis [2]. Plasmons refer to the collective vibrations of charge that occur at the boundary among the dielectric and metallic substances. These vibrations result in the generation of highly strong local fields in the surrounding area of charged particles. The phenomenon of collective charge oscillations occurring at the outermost interfaces, commonly referred to as plasmonic surface waves (PSW), can be effectively guided over the interface in the form of a propagating wave called surface plasmon polariton (SPP) [11]. SPPs are being designed and controlled between metal and dielectric interfaces in such a way so that most of the optical power is transformed from core-guided mode to SPP modes which result a sharpened resonance peak to execute resonance phenomena in the group XI materials of periodic table [3]. SPPs can be created between metal and dielectric interfaces by coupling the electromagnetic field into highly charged particles of plasmonic materials, such as gold, silver, copper, and aluminum. To produce an intense excitation of plasmon waves on the PCF surface, the appropriate choice of plasmonic materials is also crucial. As a result of its sharpened resonance peak and not having an inter-band transition, Silver is said to be a great plasmonic substance. However, the material's excessive oxidation properties prevent its broad use in aqueous environments. On the other side, gold shows a significant shift in the resonance peak and is a chemically durable metal [3]. Internal and external are two sensing mechanisms in terms of placement of the analyte inner or outer surface of the PCF. Internal sensing mechanisms are difficult in real-time detection. The disadvantages of the internal sensing strategy can be overcome by external sensing, which is why it is chosen. Researchers focused on PCF-based SPR sensors utilizing tunable optical properties of PCFs for improving the sensitivity of the label-free detection capability of SPR sensors. A PCF-based dual-core SPR sensor was suggested by Mahfuz et al. where a maximum wavelength sensitivity wavelength sensitivity (WS) of 28,000 nm/RIU was achieved within the RI range of 1.33-1.42 [4]. Hasan et al. [5] presented a dual-polarized spiral PCF sensor, where the highest WS was 4600 nm/RIU and the maximum amplitude sensitivity (AS) was 420.4 RIU^{-1} for the analytes ranging from 1.33-1.38. By optimizing geometry parameters, the highest WS of 25000nm/RIU and AS of 1411 RIU^{-1} for the samples ranging from 1.33-1.38 was proposed by Islam et al. [6]. All the recently published articles [4]–[6] were capable of detecting a single analyte at a time and also, the sensing range is narrow. Multi-analyte detection approach has gained interest in detecting multiple analytes at a time due to its rapid detection capacity and cost-efficiency. A small number of articles were published related to the multi-analyte approach in recent years. Articles [7], [8] have shown better performance in terms of WS and AS, where multiple analyte detection techniques have been addressed. However, the sensing ranges of those published articles related to multi-analyte were very narrow. In what follows, multianalyte detection schemes require to study further and open a new horizon of research nowadays [8].

This manuscript proposes a PCF-based SPR sensor that has the ability to detect multiple analytes simultaneously with an

extremely wide sensing range. The design showed the highest AS of 1629 RIU^{-1} and WS of 22000 nm/RIU with an ultra-wide range of 1.17-1.43, which covers gaseous and liquid materials. Compared to recently published articles, for the first time, this model exhibited multiple analytes detection capability with a broad range of samples, which covered bio-sensing, chemical sensing, and other lower refractive indices detection applications. Since the proposed sensor covers an ultra-wide sensing range of RI, it will be a suitable candidate for LOC technology by replacing the used traditional prism-based SPR sensor.

II. DESIGN PROCEDURES OF THE PROPOSED MODEL

With fused silica serving as a backdrop material, the geometry of the suggested sensor is depicted in Fig. 1(a). The light is controlled by 14 periodic air holes surrounding the core. The optimum size of the pitch is taken at 3 µm, where the other parameters including the air hole depend on its pitch. To control the light properly, air holes with two different sizes are chosen. A layer of 40 nm gold is employed on silica in each channel that is separated by silica. Fig. 1(b) and (c) depict the core-guided mode and SPP mode light confinement, respectively.

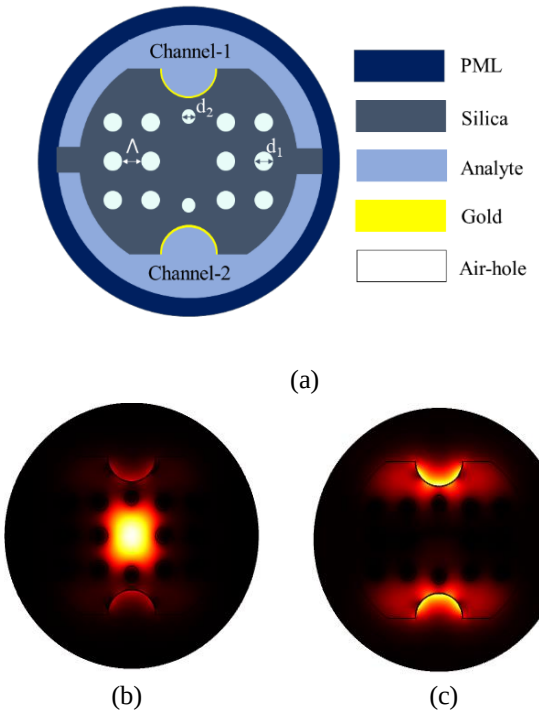

(a)

(b) (c)

Fig. 1: (a) 2-dimensional cross-sectional view, (b) and (c) are the core and SPP mode respectively

III. EQUATIONS

Different types of materials are being used to design sensors. Due to its flexibility, cheaper price, long-range transparency, and availability, fused silica is one of the most popular glass materials sensor applications. Fused silica is the PCF backdrop material, and it may be described from the Sellmeier equation [12].

$$n^2(\lambda) - 1 = \sum_{i=1}^{3} \frac{B_i \lambda^2}{\lambda^2 - c_i} \quad (1)$$

The light wavelength is expressed as λ in micrometers, and the RI of the fused silica is shown as n (λ). The given reference [13] contains the values of the Sellmeier constants (Bi and Ci). The evanescent field is essential to the SPR sensor's functioning mechanism. This evanescent field can be made even stronger by changing the structure. Strong light propagation strikes the metallic layer, causing electrons that are free on the outermost layer of metal to be stimulated. The detecting capacity of the plasmonic sensor is greatly influenced by the choice of plasmonic material. Because of its improved environmental stability and intrinsic inertness, Au is a frequently used plasmonic material.
Consequently, Au film has been chosen that is coated to the PCF sensor's outside surface. The dielectric function of gold (Au) is derived from the Drude-Lorentz model [10].

$$\epsilon_{Au} = \epsilon_{\infty} - \frac{\omega_D^2}{\omega(\omega + j\Upsilon_D)} - \frac{\Delta\epsilon\Omega_L^2}{(\omega^2 - \Omega_L^2) + j\Gamma_L\omega} \quad (2)$$

ϵ_{Au} stands for the permittivity of gold, whereas $\epsilon_{\infty} = 5.9673$ indicates the high-frequency permittivity [10]. The performance evaluation of the presented sensor is conducted by analyzing the CL properties of different analytes, which are determined using the equation [14], [15]:

$$\mathrm{CL}\left(\frac{dB}{cm}\right) = 8.868 \times k_o \times \mathrm{I_m}[n_{eff}] \times 10^4 \quad (3)$$

The symbol k_o represents the open space wave propagating number, and the operating wavelength is represented by $2\pi/\lambda$. $I_m(n_{eff})$ refers to the imaginary part of the effective mode index. The sensitivity due to wavelength shifting of the sensor is determined by applying the following equation [14]:

$$\mathrm{WS} = \frac{\Delta\lambda_{peak}}{\Delta n_a} \quad (4)$$

where Δn_a and $\Delta\lambda_{peak}$ represent the wavelength variation of the resonance peak and the RI fluctuations of the two neighboring analytes. There is an additional important investigation known as AS. When the RI level of the analytes approaches that of silica, the coupling energy increases, leading to a corresponding rise in AS. The AS can be calculated by using the following equation.

$$\mathrm{AS}(RIU)^{-1} = -\frac{1}{\alpha(\lambda, n_a)} \frac{\delta\alpha(\lambda, n_a)}{\delta n_a} \quad (5)$$

Sensor resolution (SR) is an essential parameter for assessing the ability of sample RIs to identify minor fluctuations. The SR can be calculated by using the following expression, which is taken from [10].

$$\mathrm{SR} = (RIU) = \Delta n_a \times \Delta\lambda_{min}/\Delta\lambda_{peak} \quad (6)$$

IV. SIMULATION RESULTS AND DISCUSSION

Fig. 2(a) and (b) depict the CL vs wavelength curves in the range of RI 1.17-1.43 where CL is increasing concerning wavelength, where a single analyte is used on both channels. A maximum CL of 176 dB/cm is observed at the operating wavelength of 1.20 µm at RI of 1.43, where the highest WS 22,000 nm/RIU is found for RI 1.42. AS vs wavelength, curves are demonstrated in Fig. 2(c), (d) where the highest AS is attained 1628 RIU^{-1} at RI 1.42.

Fig. 3(a) and (b) exhibit loss and AS concerning wavelength, where the RIs of Ch-1 were kept unchanged and RIs of Ch-2 were varied. Fig. 3(a) and (b) show that Ch-1 does

not exhibit sensitivity due to not changing the refractive index, whereas the other channel exposes sensitivity causing the RIs of Ch-2 to get varied.

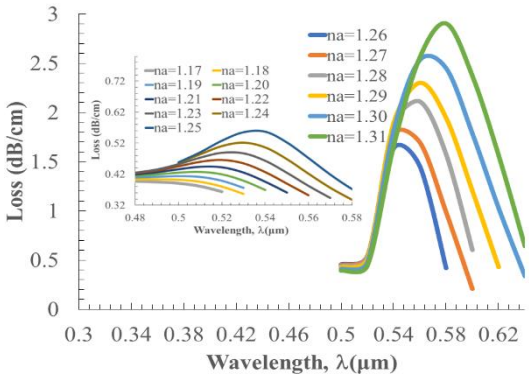

(a)

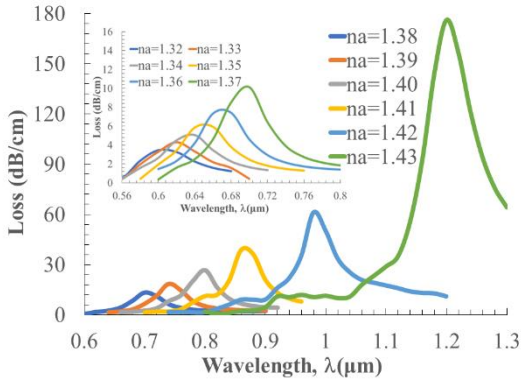

(b)

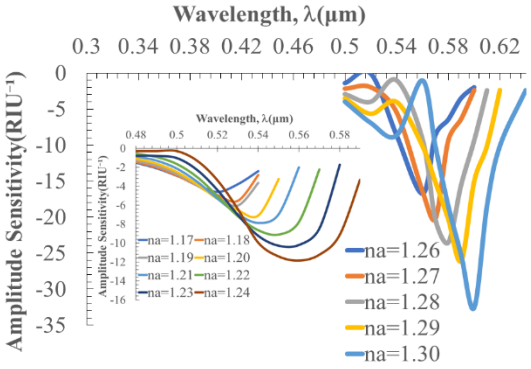

(c)

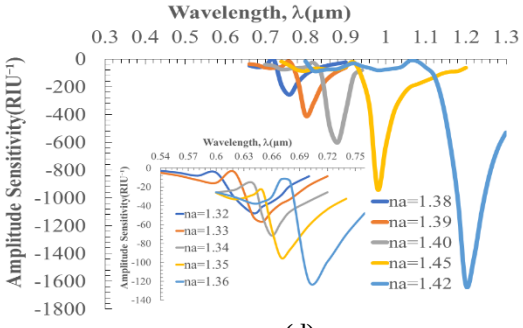

(d)

Fig. 2: (a), (b) Loss and (c), (d) AS with the change of wavelength in the range of RI 1.17-1.43, where the single analyte is used on both channels

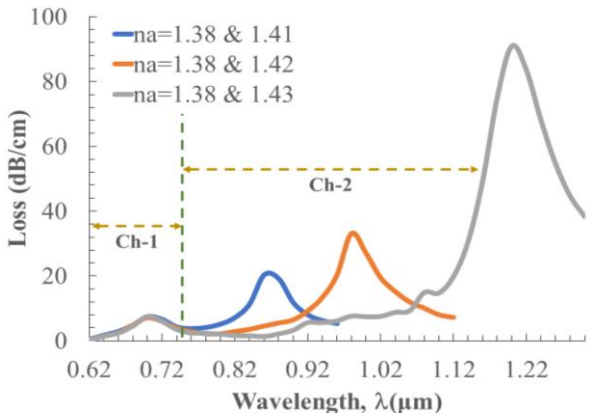

The same thing is observed in the Ch-1, where the RI of the analyte ranges between 1.38 to 1.40.

(a)

(b)

Fig. 3: (a) and (b) are loss and AS with respect to wavelength while the RI of the Ch-1 kept fixed at 1.38 while the RIs of Ch-2 are varied from 1.41 to 1.43.

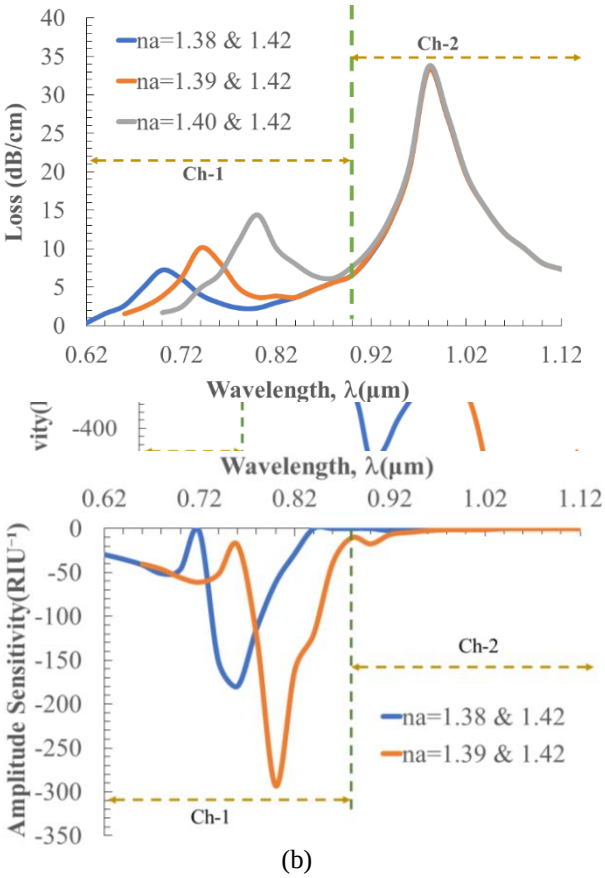

(a)

(b)

Fig. 4: The RIs of Ch-1 are changed from 1.38-1.40 where RI of Ch-2 kept same at 1.42 in Fig. (a) and (b).

As a result, the resonant wavelength gets a shift, whereas the resonant wavelengths of the Ch-2 remain constant shown in Fig. 4 (a) and (b).

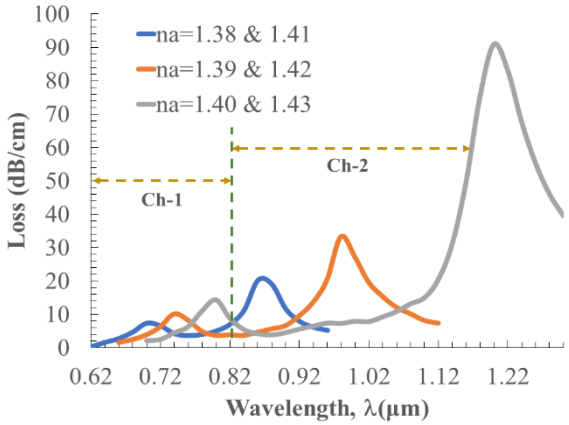

(a)

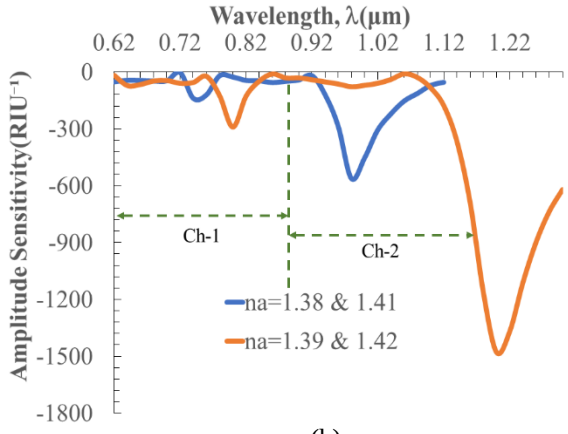

(b)

Fig. 5: RIs of both channels are varied in (a) and (b).

It is also observed that in Fig. 5(a) and (b) resonant wavelengths are shifted for both channels due to varying the RIs of both channels. The outstanding performance of the proposed model regarding WS, AS, and sensing range is investigated. compared to recent published articles [7], [8] on multianalyte detection sensors. In ref. [7], within 1.33 to 1.40 sensing range, AS and WS were found 807 RIU^{-1} and 12,000 nm/RIU, respectively whereas in ref. [8] AS and WS were reported as 1119 RIU^{-1} and 12,800 nm/RIU respectively in the sensing range of 1.33 to 1.43 RIU. The reported results of the proposed one indicate the superiority.

TABLE I: The proposed design's outcomes with the RI variation

RI	CL (dB/cm)	AS(RIU^{-1})	WS (nm/RIU)	SR ($\times 10^{-5}$)
1.17	0.39	-4.61	1000	10
1.18	0.41	-5.52	1000	10
1.19	0.42	-6.04	1000	10
1.20	0.43	-7.08	500	20
1.21	0.44	-7.87	500	20
1.22	0.46	-9.1	500	20
1.23	0.48	-10.28	500	20
1.24	0.52	-11.85	1000	10
1.25	0.56	-13.51	500	20
1.26	1.64	-16.77	500	20
1.27	1.80	-20.27	500	20
1.28	1.39	-23.51	500	20
1.29	2.30	-26.06	500	20
1.30	2.53	-32.62	500	20
1.31	2.91	-38.87	1000	10
1.32	3.45	-47.93	1500	6.67
1.33	4.33	-56.86	2000	5
1.34	5.05	-71.77	2000	5
1.35	5.94	-95.14	2000	5
1.36	7.43	-120.24	2000	5
1.37	10.14	-190.83	2000	5
1.38	13.35	-258.52	2000	5
1.39	18.49	-408.03	4000	2.5
1.40	26.62	-601	6000	1.67
1.41	38.70	-938.38	12000	0.83
1.42	61.22	-1628.21	22000	0.45
1.43	176.12	-	-	-

Table 1 displays the suggested sensor's results where CL, AS, and WS are compared with the corresponding RI. Notably, the sensor can detect a wide range of RI. So, it can be said that the sensor will be usable for LAB-on-Chip applications. On the other hand, table 2 demonstrates the comparison of recently published articles with the proposed model.

TABLE II: Comparison of recently published articles with the proposed design

Sensing Range	AS (RIU^{-1})	WS (nm/RIU)	Ref.
1.33-1.40	807	12,000	[7]
1.33-1.43	1119	12,800	[8]
1.32-1.42	2606	20,000	[9]
1.33-1.42	427	18,000	[10]
1.17-1.43	1629	22,000	Proposed

V. CONCLUSION

The proposed model showed maximum WS (22000 nm/RIU) and AS (1628 RIU^{-1}) at RI of 1.42 and the wide range of RI (1.17-1.43). This high sensitivity of the proposed multi-analyte detection sensor may be used to remove the constrain of limited sensitivity of level-free detection capability of traditional SPR sensors in LOC application.

REFERENCES

[1] E. Haque, M. A. Hossain, Feroz Ahmed, Y. Namihira"Surface Plasmon Resonance Sensor Based on Modified D-Shaped Photonic Crystal Fiber for Wider Range of Refractive Index Detection," IEEE Sens. J. 18, 8287-8293 (2018).

[2] C. ¨I. Kuru, F. Ulucan-Karnak, S. Akg¨ol"4 - Lab-on-a-chip sensors: recent trends and future applications," Principles and Novel Designs, 65-98 (2023).

[3] E. Haque, M. A. Hossain,Y. Namihira, Feroz Ahmed, "Microchannel-based plasmonic refractive index sensor for low refractive index detection," Appl. Opt. J. 58, 1547-1554 (2019).

[4] M. A. Mahfuz, M. A. Hossain, E. Haque, N. H. Hai, Y. Namihira, Feroz Ahmed, "Dual-Core Photonic Crystal Fiber Based Plasmonic RI Sensor in the Visible to Near-IR Operating Band," IEEE Sens. J. 20, 7692-7700 (2020).
[5] M. R. Hasan, S. Akter, A. A. Rifat, S. Rana, K. Ahmed, R. Ahmed,R. Ahmed,H. Subbaraman,D. Abbott, "Spiral Photonic Crystal Fiber-Based Dual-Polarized Surface Plasmon Resonance Biosensor," IEEE Sens. J. 1, 133-140 (2018).
[6] M. S. Islam, C. M. B. Cordeiro, J. Sultana, R. A. Aoni, S. Feng, R. Ahmed,M. Dorraki,A. Dinovitser, B. W. NG, D. Abbott, "A Hi-Bi Ultra-Sensitive Surface Plasmon Resonance Fiber Sensor," IEEE access 7, 79085-79094 (2019).
[7] F. Haider, M. Mashrafi, R. A. Aoni,R Haider, M. Hossen, T. Ahmed, G. A. Mahdiraji,R. Ahmed, "Multi -Analyte Detection Based on Integrated Internal and External Sensing Approach,"IEEE T NANOBIOSCI 21, 29-36 (2021).
[8] A. Islam, F. Haider, R. A. Aoni, M. Hossen, F. Begum, R. Ahmed, "U-grooved dual-channel plasmonic sensor for simultaneous multi-analyte detection," JOSA B 38, 3055-3063 (2021).
[9] K. Ahmed, R. Amin, F. M. Bui, L. Chen, N. Mohammadd, F. Zahrani, S. Kumar, "Design and Analysis of Multi-Analyte Detection based Biosensor in the Visible to Near-Infrared (VNIR) Region," IEEE T NANOBIOSCI, (2023).
[10] Haider, Firoz, Rifat Ahmmed Aoni, Rajib Ahmed, Ghafour Amouzad Mahdiraji, Mohd Fahmi Azman, and Faisal Rafiq Mohamad Adikan, "Mode-multiplex plasmonic sensor for multi-analyte detection," Optics Letters 45, 3945-3948 (2020).
[11] Mohammadd, Noor, Ruhul Amin, Kawsar Ahmed, and Francis M. Bui, "Plasmonic Nanomaterials in Sensors," Biosensors Nanotechnology , 185-200 (2023).
[12] Amin, Ruhul, Lway Faisal Abdulrazak, Enam Khan, Kawsar Ahmed, Francis M. Bui, and Fahad Ahmed Al-Zahrani, "Inspection of an HSH-PCF for optical Communication with high Non-linearity, birefringence and negative dispersion," Alexandria Engineering Journal 61, 11139-11147 (2022).
[13] Amin, Ruhul, Rana M. Taha, Baraa Riyadh Altahan, Noor Mohammadd, Kawsar Ahmed, Francis M. Bui, Fahad Ahmed Al-Zahrani, and Shobhit K. Patel, "FEA LiNbO3: Finite element analysis of novel LiNbO3 material-based fiber for optical communication properties of nonlinear applications," Alexandria Engineering Journal 61, 12915-12923 (2022).
[14] Amin, Ruhul, Md Enam Khan, Lway Faisal Abdulrazak, Fahad Ahmed Al-Zahrani, and Kawsar Ahmed, "Design of novel models for optical communication with ultra-high nonlinearity, birefringence and low loss profile," Physica Scripta 96, 125107 (2021).
[15] Haque, Emranul, Abdullah Al Noman, Md Anwar Hossain, Nguyen Hoang Hai, Yoshinori Namihira, and Feroz Ahmed, "Highly sensitive D-shaped plasmonic refractive index sensor for a broad range of refractive index detection," IEEE Photonics Journal 13, 1-11 (2021).